THE INFLUENCE OF THE TRACTION FORCE DUE TO INERTIA OF THE BRAIN MASS ON TRAUMATIC BRAIN INJURY DURING SUV-TO-PEDESTRIAN IMPACT

Atsutaka Tamura[a], Yuko Nakahira[a], Masami Iwamoto[a], Isao Watanabe[a], Kazuo Miki[a], Shigeki Hayashi[b] and Tsuyoshi Yasuki[b]
[a]Biomechanics Lab., Toyota Central R&D Labs., Inc., Yokomichi Nagakute, Japan
[b]Advanced CAE Div., Toyota Motor Corporation, Toyota-cho, Toyota City, Japan

ABSTRACT

The objective of this study is to present a potential mechanism for traumatic brain injury resulting from a lateral blunt impact to the head during SUV-to-pedestrian impact. We developed an AM50th percentile model of the human head, and the mechanical response predicted by the model was validated against available cadaveric test data. It was found that the traction force due to the inertia of the brain mass plays a key role in brainstem lesion prior to the primary contact as well as the local stress/strain distribution around the lateral ventricle immediately after the contact with a vehicle.

Keywords: Brain injury, Angular acceleration, Inertia, Spinal cord, Pedestrian

IN RECENT YEARS, the fatality rate as well as the probability of serious head injury in pedestrians has been increasing as the type of passenger vehicles on public roads has shifted from a fleet populated by sedans to one represented by larger cars (Lefler and Gabler, 2004) such as light track vehicles (LTVs) and sport-utility vehicles (SUVs). Since the pattern of pedestrian injury is largely dependent on the vehicle front structure, the vehicle mass, and its traveling speed at the moment of impact, the injured body region and the injury frequency associated with car-to-pedestrian impact have gradually been changing while traumatic brain injury (TBI) is still the leading cause of morbidity and mortality in highly motorized countries. Over the past several years, to acquire a better understanding of injury mechanism, many research groups have developed finite element models of the human head and have simulated a typical TBI profile by applying translational as well as rotational acceleration pulses to the center of gravity (CG) of the head. However, the validity of these computational studies is subjected to certain limitations in the boundary conditions; these stem from a lack of information on internal and external factors derived from real-world accidents. On the other hand, full-scale pedestrian impact tests have been conducted using PMHS (postmortem human subject) and pedestrian dummy to investigate the global response and kinematics, though, it is difficult to gain the deeper insight into the intracranial brain injury. In this study, therefore, the attempt was made to directly simulate SUV-to-pedestrian impact using both a human whole-body model and a full-scale vehicle model so that potential injury mechanism of TBI can be analyzed.

METHODS

The newly developed human brain model comprises three major parts, i.e., a cerebrum, cerebellum, and brainstem, whereas the head model, including the bony structures and soft tissues, comprises 40,430 nodes and 49,694 elements in total. Additionally, a lateral ventricle was created using hexahedron elements, and cerebrospinal fluid (CSF) was modeled using solid elements to fill both the ventricular and subarachnoid spaces. The mechanical properties assigned to the head model were determined with reference to previous studies (Zhang et al., 2001; Aimedieu et al., 2004) as summarized in Tables 1 and 2. Further, a tiebreak contact definition was introduced between the dura mater and the arachnoid so that the sliding effect between these two layers could be taken into account, while a tied contact definition was used for the brain-skull interface. Since car-to-pedestrian impact is closely related to the lateral impact to the head, we validated the head model against available cadaveric test data in terms of the local point of view as well as the global point of view prior to conducting a pedestrian impact simulation. In this study, data were analyzed using the nonlinear explicit finite element solver, LS-DYNA ver. 970 (Livermore Software Technology Corp., CA, USA).

Table 1 : Material properties used in the head model

	Density (kg/m^3)	Elastic modulus (MPa)	Poisson's ratio
Cortical bone	2120	14900.0	0.22
Cancellous bone	1000	1640.0	0.30
Dura mater	1133	70.0	0.45
Arachnoid	1000	1.1	0.40
Pia mater	1000	1.1	0.40
Falx	1133	31.5	0.45
Tentorium	1133	31.5	0.45

Table 2 : Material properties used in the brain model

	Density (kg/m^3)	Shear modulus (kPa)		Decay constant (s^{-1})
Cerebrum	1000	G_0	10.0	100
		G_∞	5.0	
Cerebellum	1000	G_0	12.5	100
		G_∞	6.1	
Brainstem	1000	G_0	22.5	100
		G_∞	4.5	
CSF	1000	K	2.1 (GPa)	

RELATIVE BRAIN MOTION INSIDE THE CRANIUM DURING HEAD ROTATION

Relative brain motions with respect to the skull during multiple head rotation profiles were compared with the test results in which impacting directions were employed to simulate blows to the occipital, frontal, and lateral regions (Hardy et al., 2001; King et al., 2002). In the head impact tests, the head and neck were removed from unembalmed cadaveric specimens at the level of the second thoracic vertebra. Two columns of five to six neutral density targets were then implanted in the temporoparietal and occipitoparietal regions. The brain target motions were captured by an x-ray system during impact while the isolated specimens were attached to a specially designed suspension fixture in an inverted position that allowed both rotational and translational motions. To validate the model against these cadaveric brain motion data, the skull was considered as a rigid body so that the six components of the linear and angular acceleration pulses can be prescribed to the CG of the head. Additionally, 10 or 12 nodes in approximately the same position as the experimental targets were identified, and their nodal displacements were calculated on the basis of the CG of the model as shown in Figure 1 (Zhang et al., 2001). In the current study, three simulation experiments were performed as listed in Table 3.

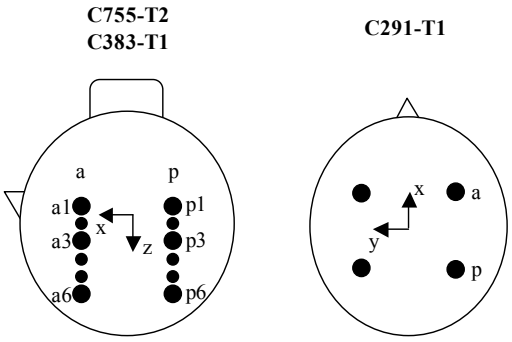

Figure 1: Brain target locations in the specimen

Table 3 : Summary of assigned acceleration pulses

Test #		C755-T2	C383-T1	C291-T1
Impact type		Occipital	Frontal	Lateral
Linear accel. (m/s^2)	X	206 -78	49 -451	108 -78
	Y	29 -69	59 -20	363 -20
	Z	98 -137	196 -402	108 -216
Angular accel. (m/s^2)	X	121 -342	395 -407	3200 -7700
	Y	1882 -574	2592 -1930	1600 -1500
	Z	60 -204	875 -523	500 -1900

LATERAL HEAD IMPACT SIMULATION

The mechanical response of the human head model to the temporoparietal impact was also compared to the experimental test results obtained by using unembalmed PMHS specimens that were isolated at the level of the occipital condyles (Yoganandan et al., 2004). These authors provided force and acceleration corridors at different velocities using free-fall techniques by impacting the specimens onto a force plate from which the forces were recorded; a 50-mm thick 40-durometer padding was used for covering the force plate. In the current simulation setup, a finite element model of the head was similarly impacted using drop techniques onto the padding material (50-mm thickness) that served as the impacting boundary condition by prescribing initial velocities of 3.5, 4.9, and 6.0 m/s (Figure 2). The reaction force generated between the temporal region of the head and the padding material was compared with the force-time traces recorded by a load cell; these traces were mass scaled to medium anthropometric dimensions according to a standard procedure employed in impact biomechanics.

SUV-TO-PEDESTRIAN IMPACT SIMULATION

The head model was then incorporated with an AM50th%ile pedestrian model ver. 1.4 of THUMS (Total Human Model for Safety) in which the brainstem was smoothly connected to the torso using the spinal cord. Thereby, the local response of intracranial brain motion as well as pedestrian kinematics during impact can be obtained. Since the majority of pedestrians are struck laterally with their lower extremities positioned in a gait-like orientation (Kam et al., 2005), the pedestrian model was positioned laterally in a similar manner along the vehicle center line in a mid-stance position (Kerrigan et al., 2005), as shown in Figure 3. In the current study, SUV-to-pedestrian impact simulation was performed with the striking vehicle traveling at 40 km/h with the deceleration pulse of 1.0 G. Subsequently, the same scenario was simulated after deleting the elements belonging to the upper part of the cervical cord to assess the influence of the traction force on the local stress/strain distribution inside the cranium during head rotation.

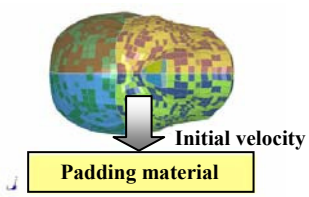

Figure 2: Setup for head drop test simulation

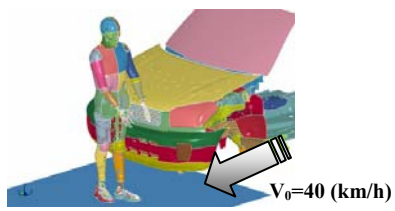

Figure 3: SUV-to-pedestrian impact simulation

RESULTS

VALIDATION OF LOCAL BRAIN MOTION INSIDE THE CRANIUM DURING HEAD ROTATION

Figure 4 shows the excursions of the brain targets predicted for occipital (C755-T2), frontal (C383-T1), and lateral (C291-T1) impact in which the magnitude of each target path was found to correlate reasonably well with the experimental data. Although some of the target paths were indicating drift compared to the observed loop shapes, this could be attributable to individual biological differences.

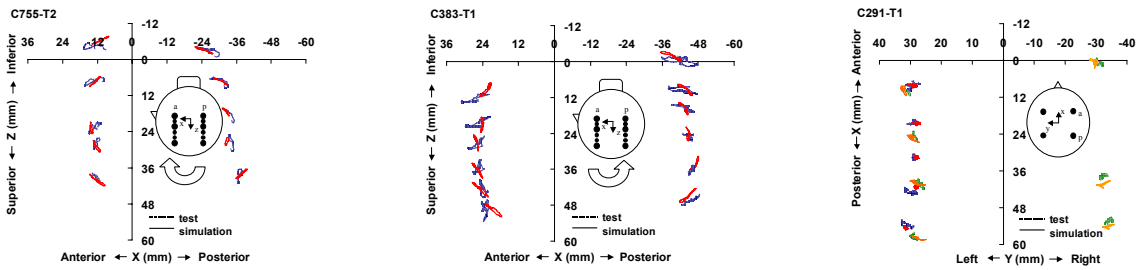

(a) Occipital impact (b) Frontal impact (c) Lateral impact

Figure 4: Comparison of local brain motion in sagittal planes (C755-T2, C383-T1) and coronal plane (C291-T1)

VALIDATION OF THE GLOBAL HEAD RESPONSE TO TEMPOROPARIETAL IMPACT

A series of simulations of temporoparietal impact to the isolated head model were carried out, the mechanical response of which was also found to be comparable to the experimental test results. The calculated resultant forces ranged from 4.8 to 10.2 kN, and although some of the tested specimens sustained fractures during dynamic loading, the simulation results did not show any sign of bony fracture of the cranium. As described earlier, a dynamic mode of loading was employed in this study to simulate real-world events that are often seen in car-to-pedestrian impact using free-fall (drop) techniques. The time history data of the reaction force and acceleration were calculated against the assigned input impact velocities of 3.5, 4.9, and 6.0 m/s. Figure 5 shows the peak resultant force and the peak acceleration responses measured at the occipital site as a function of impact velocity expressed as the mean ± one standard deviation. It should be noted that peak resultant accelerations were filtered at a channel frequency class (CFC) of 1000 Hz.

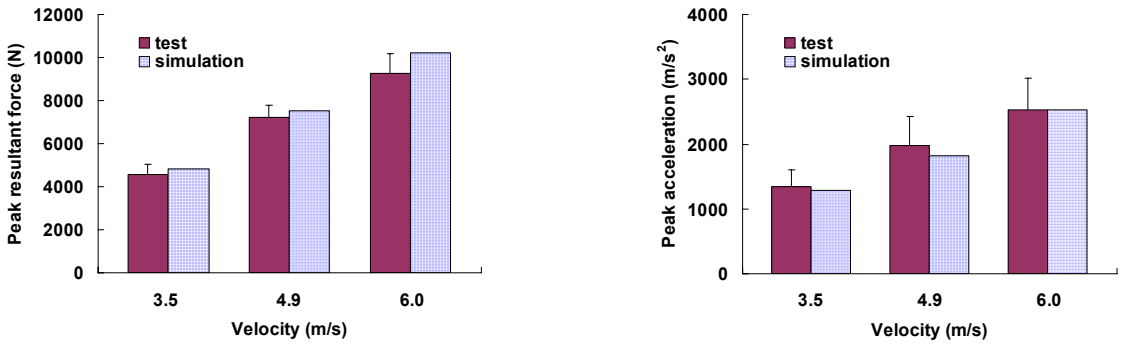

(a) Peak resultant force (b) Peak acceleration measured at the occipital site

Figure 5: Peak resultant force and acceleration as a function of impact velocity (mean ± SD)

APPLICATION OF THE HEAD MODEL TO SUV-TO-PEDESTRIAN IMPACT

Some of the previous studies have attempted to reconstruct a typical profile of diffuse axonal injury (DAI) by applying a devastating rotational angular acceleration to the CG of the head. However, it was found that the head was more readily rotated around the lower level of the cervical spine than around its CG, and the maximum angular acceleration calculated around its CG was relatively moderate, nearly 7,500 rad/s^2. On the other hand, the traction force generated due to inertial loading by head rotation prior to the primary contact with the vehicle, the resultant magnitude of which was measured at the site immediately below the occipital condyle, exceeded 90 N. Additionally, it was found that the local strain distribution around the vicinity of the lateral ventricle immediately after contact was greatly affected by this traction force as shown in Figure 6. This is because the spinal cord plays a significant role in constraining the intracranial brain motion during dynamic head rotation, and it resulted in relative difference of brain deformaion between the lower part of the cerebrum and the upper part of the cerebrum each of which was restricted by a spinal cord and falx, respectively. It is interesting to note

that strain was selectively concentrated in the corona radiata and upper brainstem, both of which are common sites of DAI (Anderson et al., 2003).

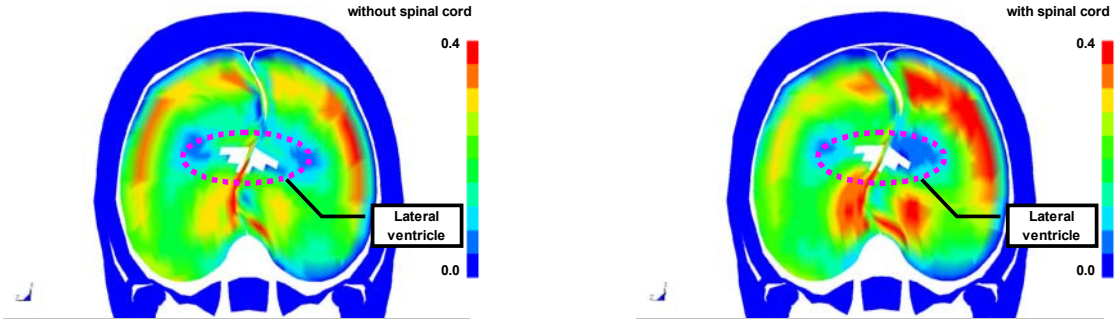

Figure 6: First principal strain distribution immediately after the primary contact (coronal section at 120 ms)

DISCUSSION

Brainstem lesion is a specific type of severe brain injury often seen in car-to-pedestrian impacts that occur independently of head impacts (Gunji et al., 2002). In this study, the possible mechanism of traumatic brainstem injury was proposed to entail an inertial loading due to head rotation during free flight that causes a traction force in the spinal cord; this produces a resultant force in excess of 90 N, in spite of the fact that the brain mass of an adult male does not exceed 1.5 kg. The rotational angular acceleration of 7,500 rad/s^2 along with the angular velocity of 30 rad/s observed around the CG of the head immediately after the primary contact appears to be relatively moderate in comparison with the threshold for DAI proposed by Margulies and Thibault (1992). The local principal strain around the vicinity of the lateral ventricle, however, was in excess of 40%; this value far exceeds the tissue-level thresholds predicted for DAI (Bain et al., 2000). As described earlier, the traction force produced in the spinal cord plays a significant role in constraining the brain motion inside the cranium. These results suggest that, to accurately assess the probability of TBI inside the skull, we should focus on the global response as well as the local brain deformations that are readily affected by the boundary conditions. The current study was limited by our experimental approach; that is, we employed a linear viscoelastic material model to represent the mechanical properties of brain tissue, which is essentially an anisotropic, nonlinear, and incompressible material. Additionally, validity of the global response in lateral head motion is limited due to a lack of quantified information of the human head in side impacts. Another limitation is a pedestrian position. Since we focused on lateral impact situation in this study, the potential effect of neck extension on brainstem injury might be precluded. In the future, we will attempt to specify potential injurious factors for DAI by changing the vehicle type, pedestrian position, and impacting speed.

CONCLUSIONS

A human head model was developed and the mechanical responses of this model were validated against available cadaveric test data in terms of both local and global points of view. We then applied the model to an SUV-to-pedestrian impact simulation to elucidate the effect of the spinal cord on TBI. It was found that one of the possible injury mechanisms associated with pedestrian impact is the traction force due to the inertia of the brain mass; this force appears to contribute to TBI in two phases, i.e., the inertial loading during free flight resulting in a brainstem lesion, and the potential constraining effect on the intracranial brain motion immediately after the primary contact. We believe that the delay of the stress/strain propagation observed between the cerebral surface and the vicinity of the lateral ventricle is more readily affected by a boundary condition in the second phase, and that this condition is primarily responsible for the injury mechanism in DAI.

REFERENCES

Aimedieu P. and Grebe R. (2004) Tensile strength of cranial pia mater : preliminary results., J Neurosurg. **100**, pp. 111-114.
Anderson R.W.G., Brown C.J., Blumbergs P.C., McLean A.J., and Jones N.R. (2003) Impact mechanics and axonal injury in a sheep model, J Neurotrauma, **20**, pp. 961-974.
Bain A.C. and Meaney D.F. (2000) Tissue-level thresholds for axonal damage in an experimental model of central nervous system white matter injury., J Biomech Eng., **122**, pp. 615-22.
Gunji H., Mizusawa I., and Hiraiwa K. (2002) The mechanism underlying the occurrence of traumatic brainstem lesions in victims of traffic accidents., Legal Medicine, **4**, pp. 84-89.
Hardy W.N., Foster C.D., Mason M.J., Yang K.H., King A.I., and Tashman S. (2001) Investigation of head injury mechanisms using neutral density technology and high-speed biplanar X-ray. Stapp Car Crash Journal, **45**, pp. 337-368.
Kam C.Y., Kerrigan J., Meissner M., Drinkwater C., Murphy D., Bolton J., Arregui C., Kendall R., Ivarsson J., Crandall J., Deng B., Wang J.T., Kerkeling C., and Hahn W., (2005) Design of a full-scale impact system for analysis of vehicle pedestrian collisions., Paper 2005-01-1875, Society of Automotive Engineers, Warrendale, PA.
Kerrigan J., Kam C., Drinkwater C., Murphy D., Bose D., Ivarsson J., and Crandall J. (2005) Kinematic comparison of the Polar-II and PMHS in pedestrian impact tests with a sport-utility vehicle., In: Proceedings of IRCOBI Conference, pp. 159-174.
King A.I., Hardy W.N., Mason M.J., and Tashman S. (2002) Comparison of relative motion between the brain and skull of the human cadaver for rotation in the coronal and sagittal planes. In: Proceedings of 4th World Congress of Biomechanics, Calgary, Alberta, Canada.
Lefler D.E., and Gabler, H.C. (2004) The fatality and injury risk of light truck impacts with pedestrians in the United States, Accid Anal Prev, **36**, pp. 295-304.
Margulies S.S. and Thibault L.E. (1992) A proposed tolerance criterion for diffuse axonal injury in man. J Biomech., **25**, pp. 917-923.
Yoganandan N., Zhang J., and Pintar F.A. (2004) Force and acceleration corridors from lateral head impact. Traffic Inj Prev, **5**, pp. 368-373.
Zhang L., Yang K.H., Dwarampudi R., Omori K., Li T., Chang K., Hardy W.N., Khalil T.B., and King A.I. (2001) Recent advances in brain injury research: a new human head model development and validation. Stapp Car Crash Journal, **45**, pp. 369-394.